Use of an Ultrasonic Resonance Technique to Measure the in-plane Young's Modulus of Thin Diamond Films Deposited by a DC Plasma Jet

L.Chandra and T.W.Clyne

Department of Materials Science and Metallurgy

University of Cambridge

Pembroke Street, Cambridge CB2 3QZ, U.K.

1. Introduction

There is considerable current interest in diamond films produced by chemical vapour deposition routes[1-4]. One of the main objectives of current research in this area concerns the optimization of the growth rate of the film. One of the most promising methods of generating relatively high growth velocities involves deposition with a DC Plasma Torch[5-9], with which high impingement velocities of the plasma gas mixture on the substrate can be generated. Investigation of the relationships between deposition conditions and the deposition rates and deposit characteristics is, however, less advanced than is the case for more conventional CVD processes. In practice, many diamond films produced with a DC Plasma Jet have been somewhat impure, porous, graphitic (having a low sp^3/sp^2 bond hybridization ratio) or otherwise imperfect.

An important requirement in such studies is the quick and reproducible characterization of deposited films, preferably in such a way that a clear indication can be obtained of how closely the film approaches to the ideal of a pure and perfect diamond structure. A promising approach to this is measurement of the elastic constants of the film, since all of the defects mentioned above will reduce the stiffness. Unfortunately, accurate measurement of, for example, the in-plane Young's modulus is usually rather difficult to carry out by conventional static methods, since the films are very thin, typically much thinner than the substrate, to which they normally adhere strongly. However, there is scope for making such measurements using dynamic methods, which can be accurate and reproducible. In the present paper, an outline is given of how a simple procedure for the measurement of resonant frequency can be applied to a substrate, before and after the deposition of a thin, adherent film, so as to measure the Young's modulus of the film with a fair degree of accuracy. Some illustrative data are presented for metallic coatings produced by electrodeposition and for diamond coatings deposited using a DC plasma torch. The method does not appear to have been used previously for this purpose, although sonic velocity measurement has been employed[10] for characterisation of thermally sprayed coatings.

2. Resonant Frequency Measurements for Stiffness Determination

Various dynamic measurements[11] can be made to obtain information about material stiffness, and it has been shown[11,12] that consistent results are obtained from different methods. One of the most convenient procedures is to measure the fundamental response frequency of flexural vibration of an elongated specimen. For a prismatic beam, this vibration mode has two resonance nodes, located

about 22.4% of the specimen length in from either end[13]. For an isotropic material, the flexural modulus dictating the frequency, f, of this vibration is equal to the Young's modulus, E, of the material. The value of E is readily calculated from the following equation[13]

$$E = 0.94642 \left(\frac{\rho L^4 f^2 \Gamma}{h^2} \right) \qquad (1)$$

where ρ is the density (in kg m^{-3}), L and h are specimen length and thickness (in m), f is the resonant frequency (in Hz) and Γ is a dimensionless shape factor (dependent on specimen length, specimen width, b, and Poisson's ratio, ν). The vibration can be induced electro-magnetically or piezo-electrically[11], but one of the simplest and most effective methods is to introduce a mechanical impulse (eg. a tap with a small hammer), with the specimen supported at the two nodes, so as to encourage the induction of the fundamental vibration. This method has been applied in various situations, including operation at elevated[14] and cryogenic[15] temperatures. The technique has also been applied to (dental) composites[16] and multi-phase materials such as rocks[17], although in these cases the specimens were still treated as isotropic continuua.

3. Experimental Procedure

3.1 Electrodeposition of a Reference Metallic Film

To test the validity of the technique, two thin uniform layers of metallic nickel were electrodeposited onto copper plates, using a solution consisting of 169 g of $NiSiO_4$, 23 g of $NiCl$ and 19 g of H_3BO_3 in 1 litre of distilled water. A plating-solution temperature of about 60 °C and a plating current of 100 mA was maintained, with deposition times of about 7 and 11 hours. Deposits were formed on one side only of the plates, the other being protected by a lacquer. The average thickness of a film was established by weighing the plate before and after deposition, using a high precision microbalance ($\pm$ 10 μg). After the ultrasonic measurements had been carried out, the density of the films was established, after mechanical detachment of slivers from the substrate, by Archimedean pycnometry. This density was used in calculating the thickness of the nickel films. In order to predict the effect of porosity in the film on its elastic constants, a comparison was made between measured and theoretical density in order to establish the pore content. It was assumed that the pores were present as an array of spherical holes. The Young's modulus (and Poisson's ratio) of the film were then calculated using the Eshelby equivalent homogeneous inclusion method[18,19].

3.2 DC Plasma Deposition of Diamond Films

Diamond deposition experiments were carried out using a Plasma-Technik PT800-M1000 VPS unit. The plasma jet was generated by a standard F4-V torch with a cylindrical tungsten insert as anode and a central tungsten rod as cathode. A plasma jet was struck by passing a mixture of high purity argon, hydrogen and methane gases through the gap between the two electrodes, across which a constant current dc voltage was maintained. Mild steel plates were grit blasted and degreased prior to use as substrates for the deposition of the diamond films. Deposition conditions are given in Table I for two representative specimens. Film thicknesses were calculated from weight gain measurements, as for the nickel films. Since the diamond films were very thin, it was difficult to remove portions of them for density measurement. The film thicknesses were therefore calculated

assuming a theoretical density of 3.265 Mg m^{-3}. Clearly this will be inaccurate, particularly for highly imperfect films, but the practice is acceptable in view of the lower target precision for characterisation of the diamond films, compared with the measurements on the nickel films aimed at validation of the method.

Specimen	Ar supply (slpm)	H$_2$ supply (slpm)	CH$_4$ supply (slpm)	Substrate Temp. ($^\circ$C)	Chamber pressure (mbar)	Time (s)	Current (A)	Power (kW)	Stand-off distance (mm)
S/D1	40	1.0	0.05	880	50	20	255	10.50	100
S/D2	40	1.0	0.05	897	100	20	500	20.00	130

Table I Plasma Deposition Conditions

In order to indicate the wide range of deposit microstructures which can be produced under different conditions, two SEM micrographs are shown in Fig.1. These show general free surface views of the two deposits, which were produced under different conditions. Although it is unreliable to infer much about the detailed structure of the deposits from such images, it appears that relatively large facetted crystals are common in one of these cases, but not in the other. For both of these specimens, and for those measured ultrasonically, X-ray diffraction revealed clear (111) peaks at a Bragg angle (θ) of 21.95°, indicating the presence of at least a substantial content of diamond or a diamond-like phase. It is, however, unsatisfactory to use either X-ray spectra or micrographs in any systematic attempt to characterise the quality of diamond films.

3.3 Resonant Frequency Measurement

The measurement of resonant frequency was carried out using a "Grindosonic" machine developed by Lemmens Elektronica Ltd., with either a microphone or a contact transducer being used to sense the specimen vibration frequencies. The detection circuit[11] for the ultrasonic resonance frequency measurement device used is shown in Fig.2. Substrates were tested, with and without adherent films, by inducing vibrations with a mechanical impulse supplied by a small ball bearing. The frequency of the dominant vibration mode was displayed by the machine a few seconds after the primary excitation. Provided the nature of the dominant mode is known, this frequency can be converted to a beam stiffness using standard equations, after specifying the beam dimensions and the Poisson's ratio of the material. In the experiments described here, the substrate dimensions, specimen support arrangement and method of impulse supply were all designed to ensure that the basic beam flexure mode was dominant. It was found that this could be readily achieved. Frequency data, which could easily be collected repeatedly in a short time, were found to be highly reproducible (to four significant figures), even with variations in the precise manner of excitation. If a competitive vibration mode did become predominant, then the displayed frequency was substantially different and could be eliminated from the data collection operation.

4. Data Analysis - Bending of a Composite Prismatic Beam

The requirement is to deducethe Young's modulus, E, for a film adherent on a substrate, from the apparent E of the composite beam, knowing the dimensions and elastic constants of the substrate. The geometry is shown in Fig.3(a). The position of the neutral axis can be found by using the

condition that the resultant axial force acting on the cross section is zero. A force balance can be written

$$\int_1 \sigma_{x1}\, dA + \int_2 \sigma_{x2}\, dA = 0 \qquad (2)$$

where σ_{x1} and σ_{x2} are the normal stresses in the x direction and A is the cross-sectional area of the beam. Now, it can be seen from Fig.3(b) that the axial strain ε_x at any height y can be written

$$\varepsilon_x = \frac{(R+y)\,\theta - R\,\theta}{R\,\theta} = \frac{y}{R} \qquad (3)$$

where R is the radius of curvature and θ is the angle subtended at the centre of curvature. It follows that the axial stress is given by

$$\sigma_x = E\,\varepsilon_x = \frac{E\,y}{R} \qquad (4)$$

For a beam of width b, substitution of eqn.(4) in eqn.(2) leads to an expression involving δ, the distance of the neutral axis from the interface between the two constituents.

$$\int_{-\delta}^{H-\delta} \frac{E_1\,y}{R}\, b\, dy + \int_{-h-\delta}^{-\delta} \frac{E_2\,y}{R}\, b\, dy = 0$$

Carrying out this integration leads to

$$\frac{E_1\,b}{2\,R}\,(H^2 - \delta H + \delta^2 - \delta^2) = -\frac{E_2\,b}{2\,R}\,(\delta^2 - h^2 - 2h\,\delta - \delta^2)$$

so that δ can be evaluated from

$$\delta = \frac{E_1\,H^2 - E_2\,h^2}{2\,(E_1\,H + E_2\,h)} \qquad (5)$$

Now, the stiffness of the composite beam is defined by

$$\Sigma_c = E_1\,I_1 + E_2\,I_2 = E_1 \int_{-\delta}^{H-\delta} y^2\, b\, dy + E_2 \int_{-h-\delta}^{-\delta} y^2\, b\, dy \qquad (6)$$

which on integration leads to

$$\Sigma_c = \frac{E_1\,b}{3}\,(H^3 - 3\,H^2\,\delta + 3\,H\,\delta^2) + \frac{E_2\,b}{3}\,(h^3 + 3\,h^2\,\delta + 3\,h\,\delta^2) \qquad (7)$$

This equation can be used to establish the unknown Young's modulus E_2, since the measured resonant frequency will allow Σ_c to be calculated, provided a value can be assumed for the Poisson's ratio of the beam (needed for the constant Γ in eqn.(1)). Substitution of eqn.(5) in eqn.(7) then gives

an equation containing E_2 as the only unknown. This is a relatively complex equation, which was solved within the "Mathematica" application software on an Apple Mac computer to give the following analytical expression for E_2

$$2 E_2 = - \frac{\left(-12\,\Sigma_c + 4\,E_1\,H^3\,b + 6\,E_1\,H^2\,h\,b + 4\,E_1\,H\,h^2\,b\right)}{h^3\,b}$$

$$\pm \left[\frac{-4\,E_1\,H\left(-12\,\Sigma_c + E_1\,H^3 b\right)}{h^4\,b} + \frac{\left(-12\Sigma_c + 4\,E_1\,H^3\,b + 6\,E_1\,H^2\,h\,b + 4\,E_1\,H\,h^2\,b\right)^2}{h^6\,b^2} \right]^{\frac{1}{2}} \qquad (8)$$

For a given substrate (i.e. a specified set of E_1, H and b values), eqn.(8) can be used to evaluate the Young's modulus of the film, E_2. This is done by making experimental measurements of the resonant frequency with and without the adherent film. The resonant frequency in the presence of the film allows the effective Young's modulus of the composite beam, E_c, to be calculated from eqn.(1). The beam stiffness Σ_c is then assumed to be given by the expression

$$\Sigma_c = \frac{E_c\,(H + h)^3\,b}{12} \qquad (9)$$

This should be a good approximation, particularly when $h/H \ll 1$.

The Young's modulus of the substrate material can be calculated from the frequency when uncoated, provided the Poisson's ratio can be given as well as the substrate dimensions. For a fully dense substrate of a well-characterised material, good agreement between measured and handbook values for E_1 confirms that the specimen dimensions have been measured accurately and that the predominant vibration mode is indeed the one being assumed. It may be noted that the calculation is quite sensitive to specimen dimensions, particularly the thickness H, but relatively insensitive to the Poisson's ratio.

It is also possible to use eqn.(8) to obtain a family of curves, showing the predicted change in effective Young's modulus of the beam as a function of the actual Young's modulus of the film, for various film thickness values. Such a plot is shown in Fig.4, for a substrate with a thickness, H, of 4.71 mm and a width, b, of 31.00 mm, having a Young's modulus, E_1, of 200 GPa. These values are close to those of the steel substrates used in the present work and they give an indication of the expected sensitivity of the measured stiffness changes to the film stiffness. For example, a resolution in the measured change in E_c due to the presence of the film of, say, 0.1 GPa corresponds to an error in the inferred value for E_2 of about 160 GPa for a 1 μm thick film, whereas this falls to about 16 GPa for a 10 μm film. These figures clearly change with specimen dimensions and would be lower for a thinner substrate; in practice, however, it may be difficult to deposit films onto very thin substrates.

4. Results and Discussions

Data are shown in Table II from the measurements made on the two reference Ni-on-Cu specimens and the two experimental diamond-on-steel specimens. The densities of the copper and steel substrates were measured as 8.741 and 7.628 Mg m^{-3} respectively and the corresponding

Poisson's ratios were taken from handbook data as 0.35 and 0.30 respectively. The Poisson's ratios of the composite beams (substrate plus film) were taken as being the same as those of the corresponding substrates.

Specimen	L (mm)	b (mm)	H (mm)	f_1 (Hz)	E_1 (GPa)	h (μm)	f_c (Hz)	ρ_2 (Mg m^{-3})	film porosity (%) †	E_c (GPa)	E_2 (GPa)
Cu/Ni1	49.9	31.0	1.62	2447	117.0	28.1	2508	8.752	1.43	120.9	197.3
Cu/Ni2	50.7	31.4	1.62	2385	117.8	54.9	2531	8.804	0.85	125.3	200.1
S/D1	57.0	31.8	4.71	9843	205.1	1.9	9857	3.265*	-	206.0	940
S/D2	57.0	31.8	4.71	9728	208.2	3.9	9751	3.265*	-	209.0	534

Table II Specimen Dimensions and Ultrasonic Data

* assumed
† obtained using a measured density for a piece of reference (fully dense) pure Ni of 8.879 Mg m^{-3}.

The measured values of E_1 for copper and steel are all close to typical handbook data. This suggests that the substrate dimensions were accurately measured and the correct vibration mode was dominant. For the nickel films, the measured E_2 values are a little below handbook values for pure nickel (207 GPa). However, calculation of the expected values of E_2 using the Eshelby method, based on the measured porosity contents, led to predictions of 201.4 GPa and 203.6 GPa for specimens Cu/Ni1 and Cu/Ni2 respectively. It can be seen that these values are quite close to the measured values. It may be concluded that the measurement technique and data analysis procedure are viable for this type of application.

With regard to the measurements on the diamond films, these data are evidently preliminary and cannot be used to explore any effects of deposition conditions on film quality. Nevertheless, they do indicate both that variations in film stiffness, and hence in structure, can be detected and also that values not very far from the theoretical limit (~1000 GPa) can apparently be obtained. However, it must be emphasized that the value reported here of 940 GPa is at present subject to substantial uncertainty. In particular, it should be noted that the film concerned was a very thin one (h<2 μm), so that, referring to Fig.4, the measured change in beam stiffness would be very insensitive to the film stiffness. Taken in conjunction with the uncertainty in film density and the lack of any repeat measurements, the error in this value should probably be taken as at least 25%. Work is now in progress to obtain more comprehensive data and correlations with microstructure.

References

1. R.C. DeVries, *Synthesis of Diamond under Metastable Conditions*, Ann. Rev. Mat. Sci., vol.17 (1987), p.161-187.

2. P.K. Bachmann, *Towards a General Concept of Diamond Chemical Vapour Deposition*, Diamond and Related Materials, vol.1 (1991), p.1-12.

3. P.K. Bachmann, D. Leers and D.U. Wiechert, *Diamond Thin Films : Preparation, Characterization and Selected Applications*, Int. J. of Phys. Chem., vol.95 (1991), p.1390-1400.

4. P.R. Chalker and C. Johnston, *Overview of the Growth Methods and Mechanisms of CVD Diamond*, in "Proc. 2nd European Conf. on Adv. Mats and Procs. (Euromat'91)", (1992), T.W. Clyne and P.J. Withers (eds.), Cambridge, UK, Inst. of Materials, p.217-224.

5. K. Kurihara, K. Sasaki, M. Kawarada and N. Koshino, *High Rate Synthesis of Diamond by DC Plasma Jet Chemical Vapour Deposition*, J. App. Phys. Letts, vol.52 (1988), p.437-438.

6. K. Kurihara, K. Sasaki and M. Kawarada, *Diamond Synthesis by DC Plasma Jet CVD*, Materials & Manufacturing Processes, vol.6 (1991), p.241-256.

7. E. Lügscheider, T. Weber and W. Schlump, *General Study Associated with Diamond Synthesis by Vacuum Plasma Spraying or DC Arc Plasma Vapor Deposition*, in "4th National Thermal Spray Conference", (1991), T.F. Bernecki (ed.), Pittsburg, ASM, p.439-446.

8. N. Ohtake and M. Yoshikawa, *Diamond Film Preparation by Arc Discharge Plasma Jet Chemical Vapour Deposition in the Methane Atmosphere*, J. Electrochem. Soc., vol.137 (1990), p.717-722.

9. K.V. Ravi, *Morphological Instabilities in the Low Pressure Synthesis of Diamond*, J. Mat. Sci., vol.7 (1992), p.384-393.

10. R. Kawase, H. Haraguchi and T. Hamamoto, *Non-Destructive Evaluation Method for Thermal Sprayed Ceremic Coating Using Ultrasonic Waves*, in "4th National Thermal Spray Conference", (1991), T.F. Bernecki (ed.), Pittsburgh, ASM, p.187-191.

11. A. Wolfenden, M.R. Harmouche, G.V. Blessing, Y.T. Chen, P. Terranova, V. Dayal, V.K. Kinra, J.W. Lemmens, R.R. Phillips, J.S. Smith, P. Mahmoodi and R.J. Wann, *Dynamic Young's Modulus Measurements in Metallic Materials: Results of an Interlaboratory Testing Program*, J. Testing & Evaluation (ASTM), vol.17 (1989), p.2-13.

12. F. Aly and C.E. Semler, *Prediction of Refractory Strength using Nondestructive Sonic Measurements*, Am. Ceram. Soc. Bull., vol.64 (1985), p.1555-1558.

13. S. Spinner and W.E. Tefft, *A Method for Determining Mechanical Resonance Frequencies and for Calculating Elastic Moduli from these Frequencies*, Proc. ASTM, vol.61 (1961), p.1221-1238.

14. K. Heritage, C. Frisby and A. Wolfenden, *Impulse Excitation Technique for Dynamic Flexural Measurements at Moderate Temperature*, Rev. Sci. Instr., vol.59 (1988), p.973-974.

15. J. Zhang, A. Nyilas and B. Obst, *New Technique for Measuring the Dynamic Young's Modulus between 295 and 6 K*, Cryogenics, vol.31 (1991), p.884-889.

16. M. Braem, P. Lambrechts, V. VanDoren and G. VanHerle, *The Impact of Composite Structure on its Elastic Response*, J. Dental Research, vol.65 (1986), p.648-653.

17. R.J. Allison, *A Non-destructive Method of Determining Rock Strength*, Earth Surface Processes and Landforms, vol.13 (1988), p.1-8.

18. J.D. Eshelby, *The Determination of the Elastic Field of an Ellipsoidal Inclusion, and Related Problems*, Proc. Roy. Soc., vol.A241 (1957), p.376-396.

19. T.W. Clyne and P.J. Withers, *An Introduction to Metal Matrix Composites*, (1992), Cambridge University Press, Cambridge.

(a)
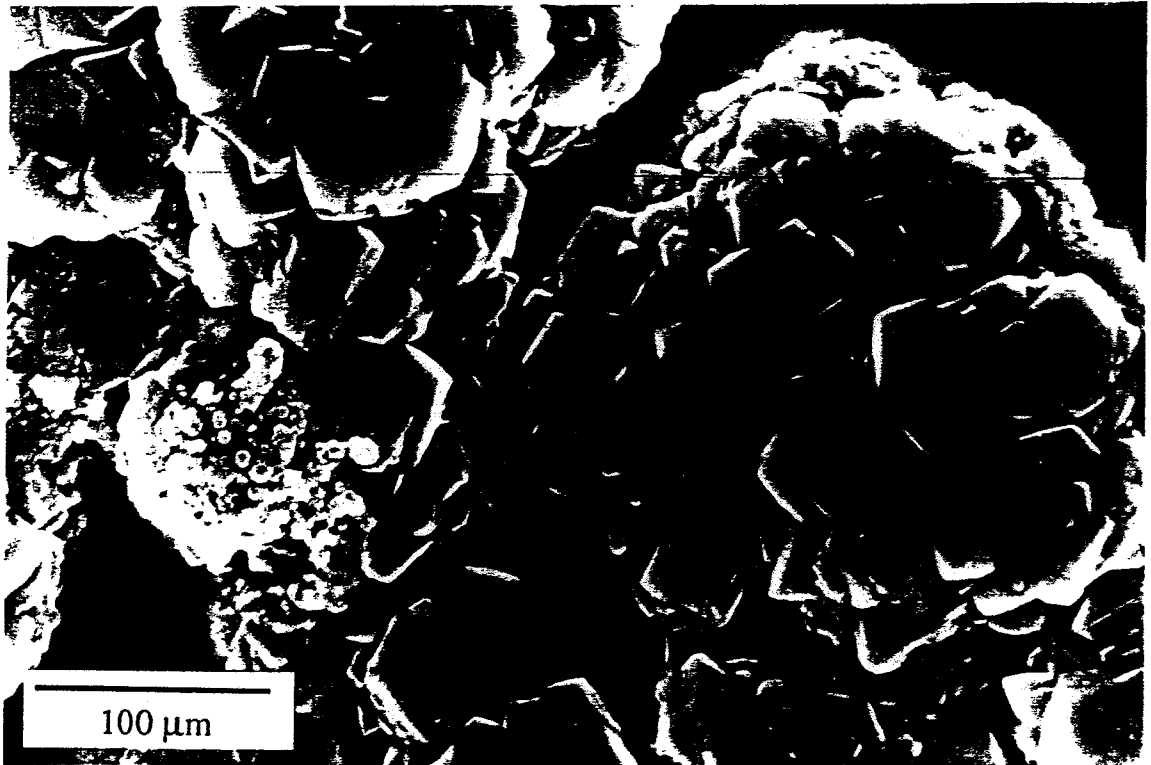
(b)

Fig. 1

SEM micrographs of diamond deposits formed on water-cooled copper substrates at 350 mbar pressure and 18 kW gun power, with (a) CH_4/H_2 ratio= 2.5% and stand-off distance = 20 mm, (b) CH_4/H_2 ratio = 1.25%, stand-off distance = 27 mm.
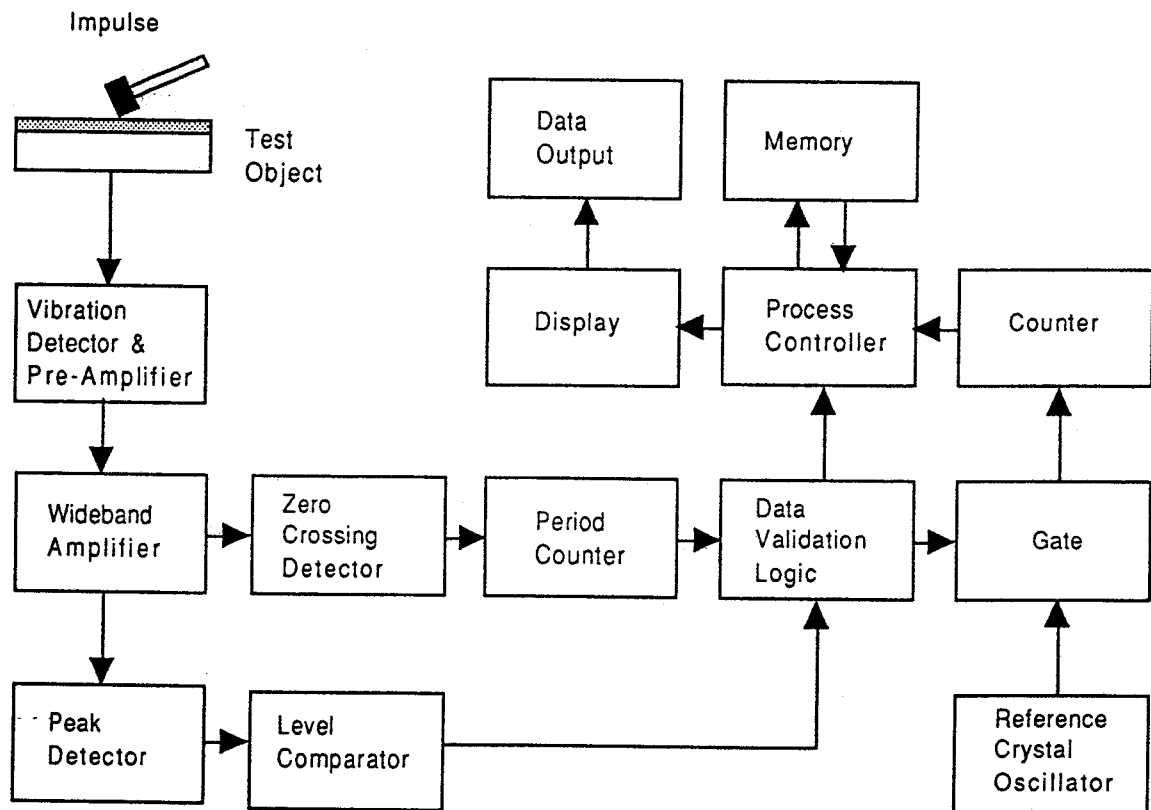
Fig.2

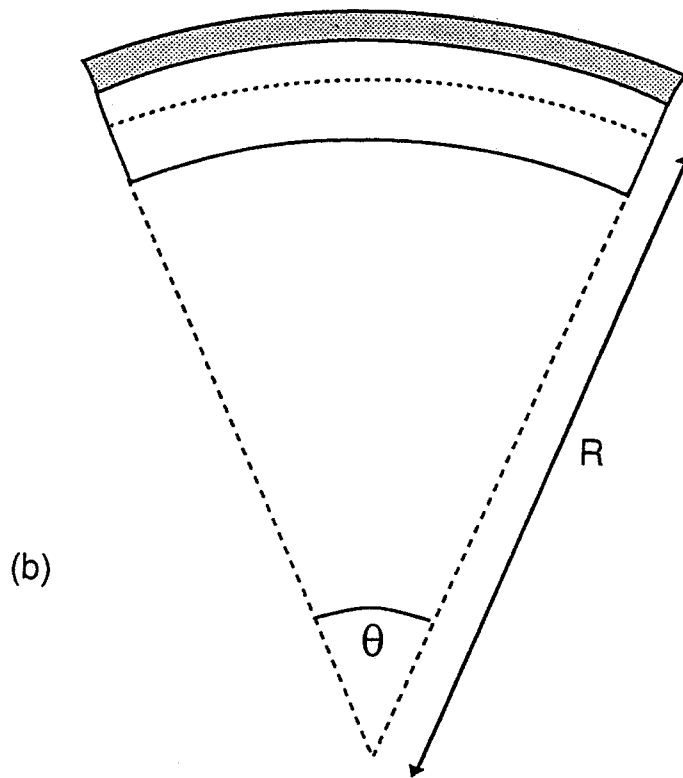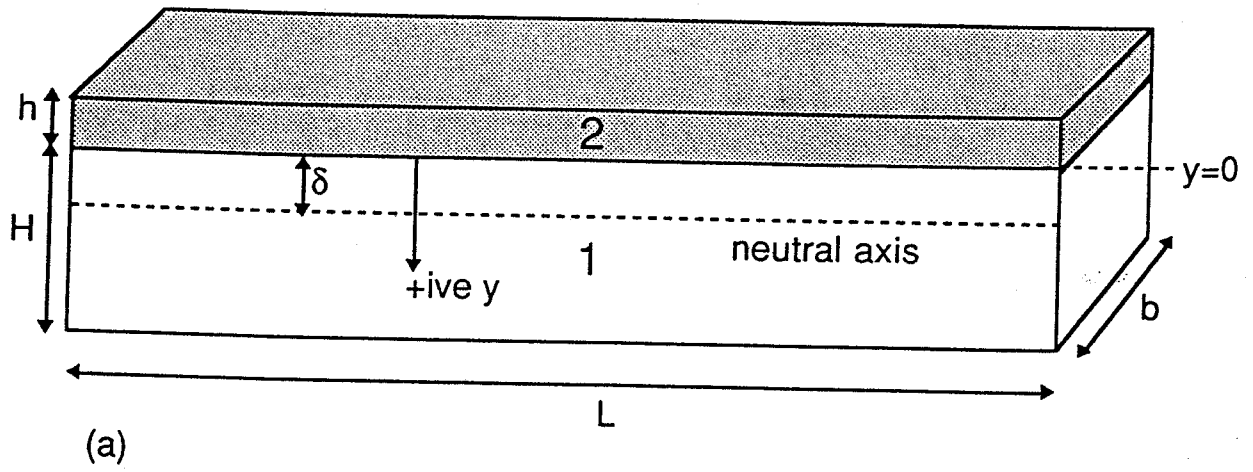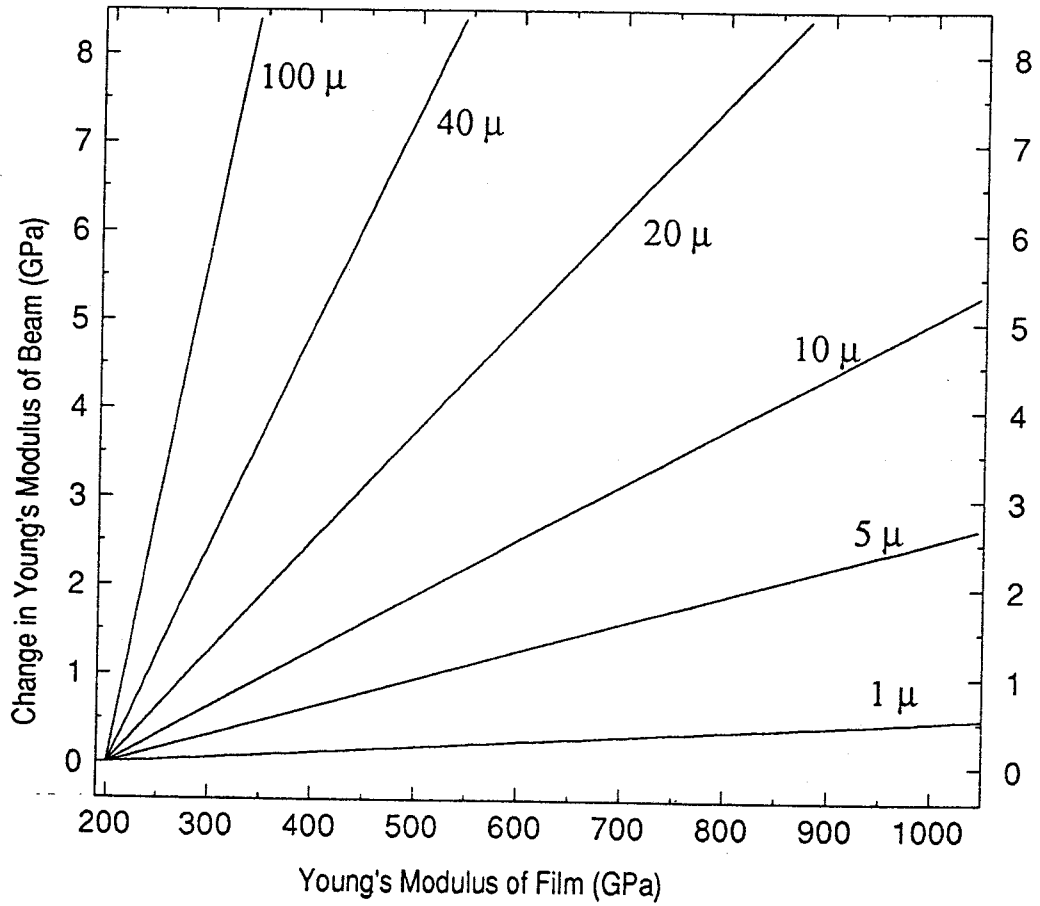Detection circuit[11] for the ultrasonic resonance frequency measurement device used.

(a)

(b)

Fig 3.

Schematic illustration of the dimensions and nomenclature for bending of a prismatic beam composed of two adherent plates of the same width and length.

Fig.4

A family of curves obtained using eqn.(8), giving the predicted change in the apparent Young's modulus of a composite beam as a function of the Young's modulus of the adherent film, for several film thicknesses. The plots refer to a substrate 31 mm wide and 4.7 mm thick, with a Young's modulus of 200 GPa.